BeBeC-2024-XX

LOCALIZATION OF SOUND SOURCES BASED ON NEAR FIELD PRESSURE

Vladimir Lebedev[1], Jan W. Delfs[2], Richard Ruck[formerly1]
[1]ebm-papst Mulfingen GmbH & Co. KG
Bachmühle 2, 74672 Mulfingen, Germany
[2]DLR, Inst. für Aerodynamik und Strömungstechnik

ABSTRACT

Recently a fundamentally new approach to localization of noise generated by a turbulent flow over a surface was introduced. This approach is based on the hypothesis that reflection of an incident pressure field on a surface does not lead to sound. This approach filters near field data by means of a diffraction filter formulated via the FW-H/Kirchhoff equation. The filtered quantity contains all the acoustically relevant surface pressure, while being orders of magnitude smaller than the hydrodynamic pressure.

Although it was only shown for high-fidelity near field data provided by a scale resolved CFD calculation, this approach is not fundamentally limited to highly resolved data. Considering recent trends in development of MEMS-based pressure sensors, surfaces may be densely covered with thousands of these and provide near field data. Because this approach is not limited to acoustic wavelengths, it can extend conventional beamforming techniques in the context of sound source localization.

This study investigates the applicability of this approach based on near field data provided by a surface covered with said MEMS. For this, an airfoil subject to a circular jet stream is considered.

1 INTRODUCTION

Modern computing resources allow the simulation of complex turbulent flows. Based on these simulations the acoustic propagation of a fluctuating surface pressure can be computed. This procedure provides a pressure-time signal in the acoustic farfield, which is comparable to a signal recorded by a microphone during an experiment.

Beamforming algorithms can be used to localize the position of sound generation. These algorithms use the pressure signals of many (virtual) microphones. The spacing of these microphones limits the resolution of the sound maps, especially for lower frequencies. Another drawback of these algorithms is the Point-Spread Function.

Looking at the procedure of beamforming in the numerical context, where first a pressure fluctuation on a surface is calculated and then propagated to the acoustic farfield, only to be used to localize a sound source on the original surface, one could pose the question, whether

the detour to the acoustic farfield is necessary, because obviously the only input to the beamforming algorithm is the surface data.

In [1],[2] an approach was introduced which directly calculates a sound map based on said surface data. It is derived from the Ffowcs-Williams and Hawkings (FW-H) equation [3] and is based on the hypothesis, that sound is only generated, where locally the mirror principle is violated.

2 DERIVATION OF THE APPROACH

For the derivation of this method the FW-H equation is used, see [3]. Assuming the integration surface to be the surface of a solid, non-moving body, neglecting the convective amplification and assuming the pressure derivative normal to the wall to be negligible the equation reduces to Eq. (1).

$$p'(\boldsymbol{x},t) = p'_f(\boldsymbol{x},t) + \frac{1}{4\pi}\int_{\partial V_B} \frac{\boldsymbol{e_r}\cdot\boldsymbol{n}}{cr}\frac{\partial p'}{\partial \tau} + \frac{\boldsymbol{e_r}\cdot\boldsymbol{n}}{r^2}p'\, dS(\boldsymbol{\xi}) \tag{1}$$

The pressure fluctuation p' at a given place $\boldsymbol{x}$ is on the left-hand side of Eq. (1). p'_f represents the volume (quadrupole) integral. The distance between the point $\boldsymbol{x}$ and a transmitter $\boldsymbol{\xi}$ is defined by $r = |\boldsymbol{r}| = |\boldsymbol{x} - \boldsymbol{\xi}|$ and the unity direction vector is $\boldsymbol{e_r} = \frac{\boldsymbol{r}}{r}$. ∂V_B is the solid surface of the body, c is the velocity of sound. $\boldsymbol{n}$ is the outwards directed normal vector of the surface element $dS(\boldsymbol{\xi})$. The integral is to be evaluated at the retarded time $\tau = t - \frac{r}{c}$.

If $\boldsymbol{x}$ is a point in the acoustic farfield, and if the flow is of low Mach number the contribution of the volume integral is negligible. However, in the nearfield it is the dominating part. Figure 1 shows a comparison of the surface pressure calculated by means of a scale resolved simulation on the left side and the sound map calculated by means of conventional numerical beamforming on the right side. Clearly, the pressure field cannot be directly used to localize the sound sources as it is dominated by hydrodynamic fluctuations which do not lead to sound generation. Analogous to Eq. (1), a separation of acoustically active and inactive parts is needed.

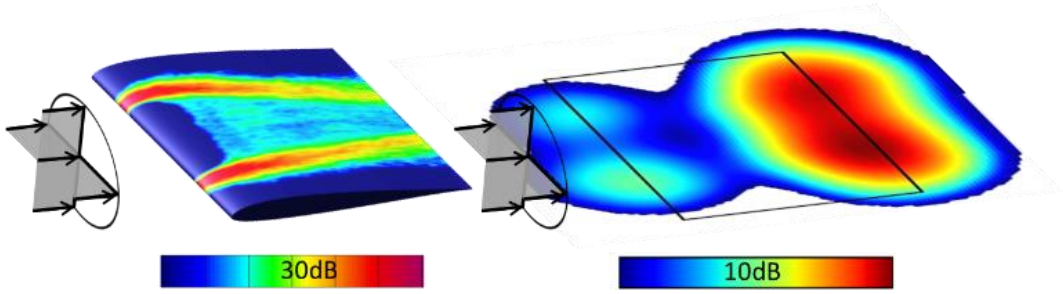

Fig. 1:2000 Hz third octave band for the pressure calculated via a scale resolved simulation (left) and the sound map calculated through numerical beamforming based on propagation of the pressure to a 56-microphone array (right).

This separation can be achieved by choosing the reception point $\boldsymbol{x}$ on the surface ∂V_B. For the point $\boldsymbol{x} = \boldsymbol{\xi}$ the integral is singular. This singularity evaluates to $2\pi p'(\boldsymbol{x},t)$, which leads to Eq. (2) with the integral to be evaluated as the Cauchy principal value.

$$\boldsymbol{x} \in \partial V_B: p'(\boldsymbol{x},t) = 2p'_f(\boldsymbol{x},t) + \frac{1}{2\pi}\int_{\partial V_B} \frac{\boldsymbol{e_r}\cdot\boldsymbol{n}}{cr}\frac{\partial p'}{\partial \tau} + \frac{\boldsymbol{e_r}\cdot\boldsymbol{n}}{r^2}p'\, dS(\boldsymbol{\xi}) \quad (2)$$

This formulation separates the reflected incident pressure from the diffracted part. To illustrate this the mirror principle shall be mentioned. It stipulates that the pressure signal for a receiver in space is influenced by the direct pressure signal p'_f from a source and the reflection at a surface. The reflection at the surface can be modeled by mirroring the source at the surface. This principle is illustrated in Fig. 2.

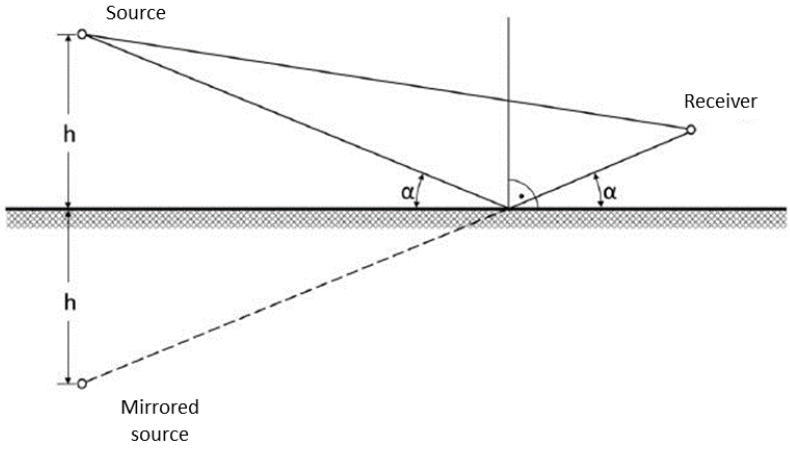

Fig. 2: Illustration of the mirror principle.

Assuming a receiver directly on the surface, the pressure signal from the mirror source is equal to the original pressure signal p'_f. This principle is formulated in Eq. (3). Comparing Eq. (2) and Eq. (3) it is evident, that the integral on the right hand side of Eq. (2) contains the fraction of the pressure that is not reflected but diffracted. The hypothesis of this approach is, that only the diffracted part of the pressure is the acoustically relevant pressure, so no sound is generated if

$$\boldsymbol{x} \in \partial V_B: p'(\boldsymbol{x},t) = 2p'_f(\boldsymbol{x},t) \quad (3)$$

The diffraction integral, which will be abbreviated as p'_s, is only dependent on the pressure on the surface, which can be calculated by means of a scale resolved simulation or by measurement of the nearfield pressure. The evaluation of the integral is analogous to a conventional propagation via FW-H, only that the propagation points $\boldsymbol{x}$ are elements of the surface, and not some farfield receiver (imagine a microphone array which is contracted towards the surface). A surface sound source term q can be formulated by inserting $p'(\boldsymbol{x},t) = 2p'_f(\boldsymbol{x},t) + p'_s(\boldsymbol{x},t)$ in Eq. (2) and reformulating it to a FW-H style equation, see Eq. (4) and Eq. (5). The quantity q describes the surface sound sources and is observer independent.

$$\boldsymbol{x} \in \partial V_B: p'_s(\boldsymbol{x},t) = 2q(\boldsymbol{x},t) + \frac{1}{2\pi}\int_{\partial V_B} \frac{\boldsymbol{e_r}\cdot\boldsymbol{n}}{cr}\frac{\partial p_s{}'}{\partial \tau} + \frac{\boldsymbol{e_r}\cdot\boldsymbol{n}}{r^2}p'_s dS(\boldsymbol{\xi}) \quad (4)$$

$$\boldsymbol{x} \in \boldsymbol{\partial V_B}: q(\boldsymbol{x},\boldsymbol{t}) = \frac{\boldsymbol{1}}{\boldsymbol{2\pi}}\int_{\boldsymbol{\partial V_B}} \frac{\boldsymbol{e_r}\cdot\boldsymbol{n}}{\boldsymbol{cr}}\frac{\partial p_f{}'}{\partial \tau} + \frac{\boldsymbol{e_r}\cdot\boldsymbol{n}}{\boldsymbol{r^2}}p'_f \boldsymbol{dS}(\boldsymbol{\xi}) \quad (5)$$

3 VALIDATION OF THE LOCALIZATION

In this chapter the localization via the diffraction filter will be compared to sound maps provided by conventional beamforming. As a test case an airfoil subject to a jet stream was chosen. The SD7003-airfoil with a chord length of 235 mm and a span of 400 mm was angled at 8° and the freestream velocity was set to 42 m/s. The airfoil's nose is placed 80 mm behind the jet nozzle exit (Ø200 mm). Because the span exceeds the jet diameter, the highly turbulent shear layers of the jet stream interact with the airfoil, see Fig. 1.

The surface data was provided by a compressible Large Eddy Simulation within the commercial software Star-CCM+. A duration of 0,1 s was simulated and the sampling rate was 100.000 Hz. The surface data was propagated to a 56-microphone array in a plane 0.72 m above the airfoil. The microphone data was then used to create sound source maps by means of conventional beamforming. Figure 3 shows the 2000 Hz third octave band for the CFD pressure (left), p_s' (middle) and q (right). The beamforming result (Fig. 1, right) and the source localization via the diffraction filter both show the dominant sources at the trailing edge of the airfoil, although the resolution and separation of each source is much better for the latter case. Especially noticeable is the difference in the dynamic range, while the beamforming result only has a range of 10 dB, the localization via diffraction filter has a range of 60 dB.

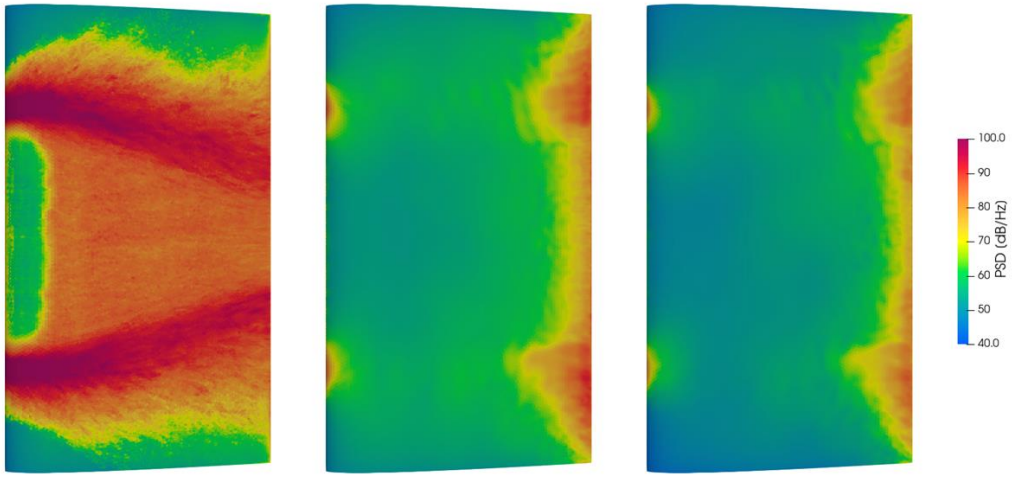

Fig. 3: 2000 Hz third octave band for the pressure calculated via a scale resolved simulation (left), p_s' calculated using the diffraction filter (middle) and q (right).

Figure 3 also shows that in most locations p_s' is four orders of magnitude smaller than p. In order to show that p_s' still contains all the acoustically relevant information, it is propagated via FW-H in to the farfield. Therefore 100 virtual microphones were placed on a circle with a diameter of 1 m around the airfoil. Figure 4 shows the directivity for the 2000 Hz third octave band for the propagation of p and p_s' (left) and the narrow band spectrum for an exemplary microphone.

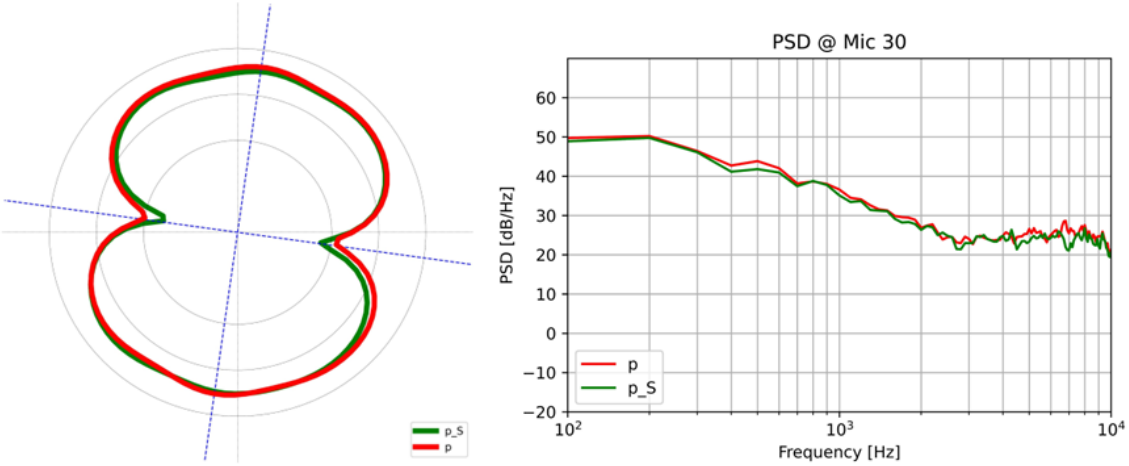

Fig. 4: Directivity for the propagation of p (red) and p'_s (green) with rotated coordinated system according to angle of attack of 8° (blue), right: Narrow band spectrum for microphone 30 (ca. 100°).

Figure 5 shows the localization for the 800 Hz third octave band. It is evident, that due to compactness the sources cannot be identified by beamforming. On the other hand, the approach through the diffraction filter is still able to separate the sources because this method is inherently not bound by any acoustic wave lengths.

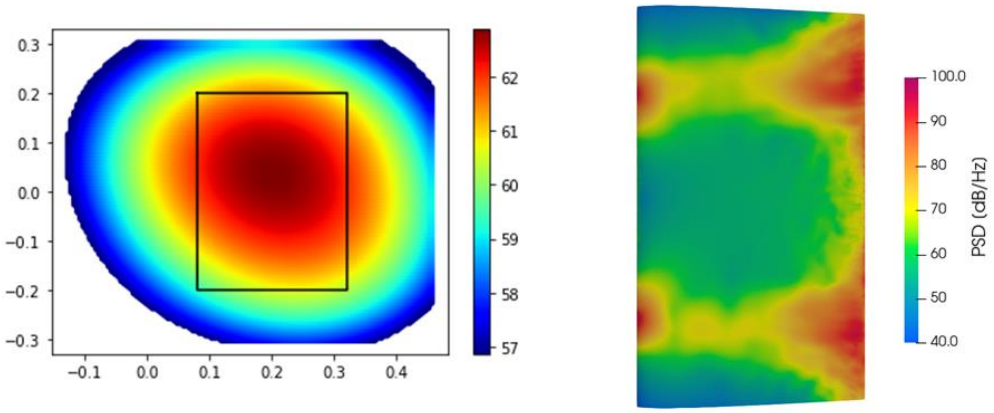

Fig. 5: 800 Hz third octave band for the sound map via beamforming (left) and p'_s via the diffraction filter (right).

4 APPLICATION WITH COARSE SURFACE DATA

The nearfield data from the scale resolved simulation was provided on a finely resolved grid. This fine resolution of the nearfield data cannot be achieved with current measurement equipment. But considering the recent development of MEMS-based pressure sensors, a somewhat resolved measurement of the nearfield of a surface is imaginable. In order to show the applicability of the method presented in this paper in the experimental context, a data set which resembles data measured by an airfoil covered with said MEMS will be used in the diffraction integral.

In order to generate the MEMS resembling data set, a rather coarse mesh for the airfoil was generated. The original mesh consisted of 87,152 triangular cells. The reduced mesh consists of 6,774 triangular cells with a distance of around 7 mm between the centerpoints. This

spacing allows a resolution of around 2450 Hz considering 20 points per wavelength. The pressure was then interpolated using the software Star-CCM+ on the coarse grid and used as input for the calculation of $p'_{s,reduced}$.

Figure 6 shows again the directivity and the narrow band spectrum for an exemplary microphone. A good agreement until the cut-off frequency around 1200 Hz can be seen between the two data sets.

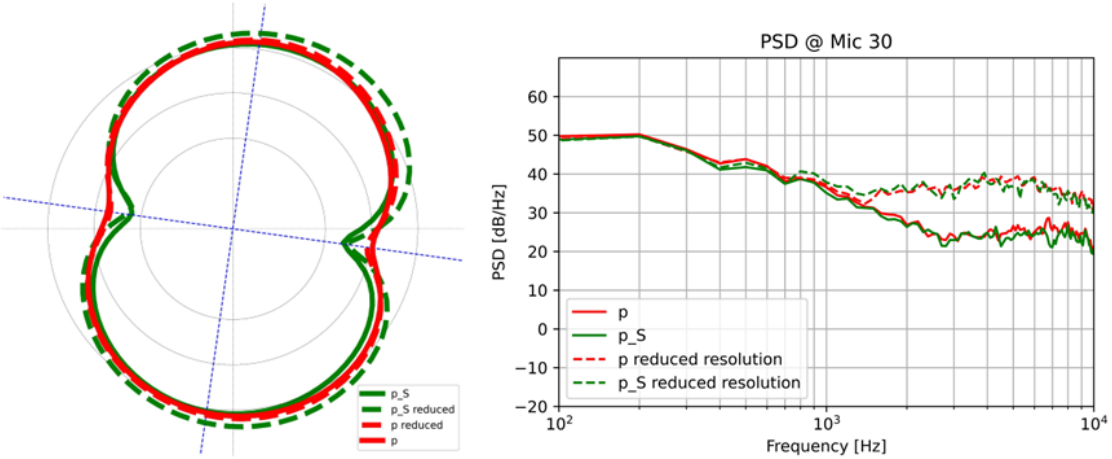

Fig. 6: Directivity for the propagation of p (red) and p'_s (green) with rotated coordinated system according to angle of attack of 8° (blue), right: Narrow band spectrum for microphone 30 (ca. 100°), dashed: propagation based on the coarse mesh.

Figure 7 shows the surface contours of p'_s and $p'_{s,reduced}$ for the 800 Hz third octave band. While the effect of the reduced resolution is clearly visible, the sound sources can still be uniquely distinguished.

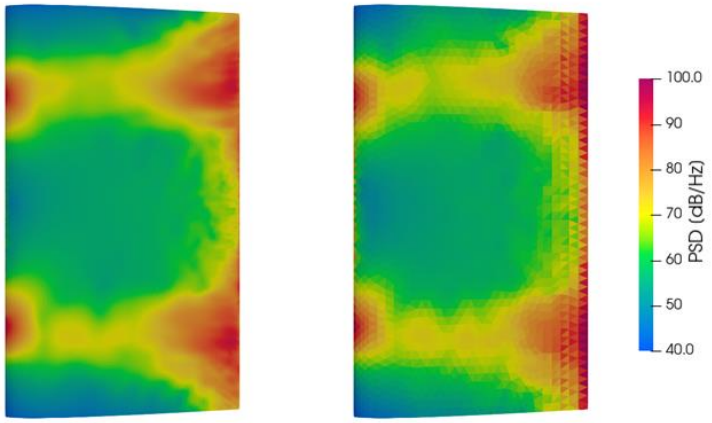

Fig. 7: 800 Hz third octave band for p'_s (right) and $p'_{s,reduced}$.

5 SUMMARY

In this paper the sound source localization via the diffraction filter was briefly presented and applied on an airfoil subject to a jet stream. The diffraction filter was derived from the FW-H equation and is based on the hypothesis, that sound is only generated, where locally the mirror principle is invalid. This way, the reflection of the incident pressure (signature of Lighthill's volume source term) is neglected and only the diffracted fraction of the pressure is left behind. The propagation of this reduced pressure showed that it truly contains all the acoustically relevant information.

Comparing the sound maps via conventional beamforming and those calculated through use of the diffraction filter showed a much better resolution using the latter. Additionally, the dynamic range is greatly increased and the resulting quantities are per definition three-dimensional and quantifiable. This filter is also not bound by any acoustic wave lengths which might be the biggest advantage to the beamforming maps.

In the first part the source data was provided on a finely resolved grid. In order to investigate the experimental use of this approach, the data was interpolated on a much coarser grid. The spacing of the grid points is close to what can be achieved with current MEMS-technology. The results for the coarse and fine data set were in good agreement until the cut-off frequency. The proposed localization approach may be particularly useful to supplement phased array techniques particularly in the low frequency range.

In the future the use of the diffraction filter needs to be investigated (and if necessary extended) for complex (and moving) three dimensional geometries.

REFERENCES

[1] Delfs, J. W., Lebedev, V., & Ruck, R. (2024). Ermittlung von aerodynamischen Schallquellen auf turbulent überströmten Oberflächen. In DAGA 2024 Conference Proceedings (pp. 1529-1532). Deutsche Gesellschaft für Akustik (DEGA)

[2] Delfs, J.W., Ruck, R. (2024). A quantity to identify turbulence related sound generation on surfaces, Journal of Sound and Vibration, Volume 586, 2024, 118490, ISSN 0022-460X, https://doi.org/10.1016/j.jsv.2024.118490.

[3] J. E. Ffowcs-Williams, D. L. Hawkings: Sound generation by turbulence and surfaces in arbitrary motion. Philosophical Transactions of the Royal Society of London. Series A, Mathematical and Physical Sciences 264 (1151) (1969), 321-342